J Biol Inorg Chem (2009) 14:1199–1208
DOI 10.1007/s00775-009-0563-z

ORIGINAL PAPER

Computational modeling of the dizinc–ferroxidase complex of human H ferritin: direct comparison of the density functional theory calculated and experimental structures

R. C. Binning Jr · Daniel E. Bacelo

Received: 11 February 2009 / Accepted: 24 June 2009 / Published online: 8 July 2009

Abstract Density functional theory optimizations of structures of dizinc(II) complexes with a six-residue model of the ferroxidase center of human H ferritin have been performed and the results compared with the crystallographically determined structure of the complex as presented in Protein Data Bank file 2CEI. The model employs the full structures of Glu27, Glu62, His65, Glu107, Gln141, and Ala144, and the structural effect of Tyr34 is also examined. The mean absolute deviation from experiment of atomic positions in the best calculated structures is less than 0.3 Å. The experimental structure is reproduced well enough to determine the coordination environment of the metal ions. Each zinc(II) center is pentacoordinate with a single water ligand, and the two centers are bridged by a hydroxide ion. Ala144 interacts weakly and repulsively with the rest of the complex. Tyr34 displays a weak attraction through a hydrogen bond to Glu107 that affects the orientation of that group.

Keywords Ferritin · Ferroxidase reaction · Density functional theory · Dizinc complex · Dimetal center

R. C. Binning Jr · D. E. Bacelo (✉)
Department of Sciences and Technology,
Universidad Metropolitana,
P.O. Box 21150,
San Juan,
PR 00928-1150, USA
e-mail: um_dbacelo@suagm.edu; dbacelo@yahoo.com

R. C. Binning Jr
e-mail: binningrc@yahoo.com

D. E. Bacelo
Departamento de Química, FCN,
Universidad Nacional de la Patagonia San Juan Bosco,
Km. 4, 9000 Comodoro Rivadavia,
Chubut, Argentina

Introduction

The mechanism of the ferritin ferroxidase reaction is complex, as are many redox reactions at metalloprotein active centers [1]. A detailed understanding of the mechanism will likely therefore require extensive, complementary theoretical and experimental efforts. A recent crystallographic study of human H ferritin (HuHF) [2] has yielded a high-resolution structure of a dizinc(II) ferroxidase complex that provides important information about the first key intermediate in the ferroxidase reaction. We report here on a density functional theoretical study of a six-residue model of this complex. The study aims to interpret important structural, bonding, and energetic properties of the complex and to examine how well the compact model represents the crystallographically determined structure.

Ferritins are the principal iron-storage proteins in animals, plants, and bacteria [3, 4]. Animal ferritins consist of 24 subunits of two types, H and L, that assemble as a hollow sphere. Although protein length and sequence vary considerably across species, three-dimensional structure is well conserved. Within each H subunit is a ferroxidase center at which two Fe^{2+} ions are bound and oxidized by O_2 to an iron(III) oxide hydrate that is subsequently transported from the center and stored in the cavity of the protein. The ferroxidase reaction is not the only path to the oxide, but it serves to initiate and accelerate oxidation [5]. The thermochemistry and kinetics of initial iron binding in HuHF have been closely examined [6, 7], and the structure of the resulting diiron(II) ferroxidase intermediate is important in interpreting the early steps of the ferroxidase reaction.

Although suitable crystals with Fe^{2+} bound in the ferroxidase center have yet to be obtained, the metal binding

positions have been identified in a number of ferritins by crystallographic analysis of native crystals soaked in various salt solutions. Both Zn^{2+} and Fe^{3+} ferroxidase complexes in *Escherichia coli* nonheme ferritin (EcFtnA) have been observed [8]. Bullfrog M (variant H) ferritin (FrMF) with Mg^{2+} [9], human mitochondrial ferritin (MtF) [10] with Mg^{2+}, Mn^{2+}, and Zn^{2+} and HuHF [2, 11–13] with Ca^{2+}, Tb^{3+}, and Zn^{2+} in the ferroxidase center have been reported. Structures of each of the above-mentioned ferritins have been lodged with the Protein Data Bank (PDB), but only in those of FrMF [9] and HuHF [2] are both metal binding sites in the ferroxidase centers occupied. In the most recent study of HuHF, structures of the wild-type center and of two mutant forms, Glu27Asp and Glu107Asp, cocrystallized with Zn^{2+} have been reported [2]. Zn^{2+} is a suitable substitute for Fe^{2+} because it is stable with respect to oxidation and reduction, the two ions are similar in size, and both are moderately Lewis acidic [14].

The amino acids essential to the binding of iron in the ferroxidase center were first positively identified in FrMF through a combination of crystallography, kinetics, and site-directed mutagenesis [15]. Site A in FrMF consists of two glutamates and a histidine in a Glu, Glu-X-X-His pattern that is common to all known H ferritins, while site B is a Glu, Gln-X-X-Asp grouping. The site B glutamate and glutamine are also conserved among H ferritins, but there is variation in the last position. The FrMF aspartate in HuHF is replaced by alanine [11], in MtF by serine [10, 16], and in EcFtnA by glutamate [8]. The site A active positions in HuHF are Glu27, Glu62, and His65, and at site B they are Glu107, Gln141, and Ala144.

Most molecular electronic structure calculations on metalloproteins employ density functional theory (DFT) when all electrons are taken into account, primarily because DFT scales more favorably with increasing molecular size than do wavefunction-based methods [17]. Two strategies of modeling are employed. The first uses as compact a model as possible, typically truncating participating amino acids to their active functional groups to simplify both the computational task and the interpretation of results [18, 19]. The second approach uses the largest possible model that is computationally feasible to include a wider range of effects. An extension of the latter approach even includes entire protein subunits by appending to the quantum mechanical treatment of the active region a molecular mechanical model of the rest of the protein, giving a quantum mechanical/molecular mechanical model [20]. Both approaches have been successful. All-electron DFT calculations on small models of dimetal centers yield accurate thermochemistry [21] when the reactions are well localized, and large model calculations provide a comprehensive view of reaction environments, including involvement of secondary ligands [22].

By far the most extensive applications of DFT to dimetal centers have been concerned with the mechanisms of reactions activating dioxygen at the diiron centers of the enzymes ribonucleotide reductase (RNR) [19, 23, 24] and methane monooxygenase [19, 25–27]. In methane monooxygenase both binding sites have the Glu, Glu-X-X-His structure seen in ferritin ferroxidase site A. Ribonucleotide reductase is similar, with one glutamate replaced by an aspartate. In fact it has been argued [9] that the ferritin center evolved from structures such as these, the introduction of Gln141 and the variations in position 144 driven by the necessity of releasing the product diiron(III) oxide from the center once it has formed.

In the present study DFT geometry optimizations are applied to the crystallographically derived geometry of the dizinc ferroxidase complex of PDB 2CEI [2]. The study aims to explain in terms of charge distribution the features of the experimental structure, in the process testing the ability of a compact model to reproduce that structure.

The model employed in this study is compact in that it is restricted to the essential ferroxidase center amino acids. However, it is necessary that full structures of these be used so that direct comparison of calculated with experimental atomic positions may be made, and that brings the sizes of the complexes treated, ranging from 105 to 137 atoms, into the category of the large models. Previous theoretical analysis of the ferritin ferroxidase reaction has been limited, but a survey of diiron(II) and diiron(III) intermediates has been done [28]. That study applied DFT calculations to a six-amino acid model similar to the one used in the present study to examine a series of intermediates between the initial diiron(II) complex and the blue peroxodiferric complex usually used to measure ferroxidase activity [29]. The resulting structures were found to be consistent in a qualitative sense with the available experimental data. The present study narrows and deepens the previous effort by attempting to define fully and as quantitatively as possible the primary coordination spheres of the metal ions of a single complex.

Methods

Energies were obtained in DFT calculations with Zn^{+2} in its ground singlet state. The BPW91 functional was employed. BPW91 employs the generalized gradient approximation with Becke's 1988 exchange functional [30] and the gradient-corrected correlation functional of Perdew and Wang [31]. Numerical basis sets of double numerical plus polarization (DNP) quality were employed. Optimizations were carried out with DMol^3 [32, 33]. During each optimization four atoms on each amino acid (two carbons, a nitrogen, and an oxygen), components of the amide-bonded backbone of

the protein, were capped where necessary with hydrogens, and fixed in their crystallographically determined [2] positions.

Results and discussion

Initial atomic coordinates for the six amino acids, one water molecule, and two zinc ions comprising the model ferroxidase center were taken from crystallographic data (PDB 2CEI) [2]. Hydrogen atoms were added, and the initial model geometry is displayed in Fig. 1. At site A, Zn^{2+} is coordinated to single carboxylate oxygens of Glu27 and Glu62, to a nitrogen on the imidazole ring of His65, and to the oxygen atom of the water molecule. Glu62 bridges sites A and B, and Zn_B is also coordinated to both carboxylate oxygens of Glu107. The amide oxygen of Gln141 is 3.82 Å from Zn_B and 3.97 Å from Zn_A. The Zn–Zn separation is 3.33 Å, and the complex has a net +1 charge.

Hydroxide bridging

BPW91/DNP geometry optimization of the model ferroxidase–zinc complex yields compound **1** (Fig. 2). In it the water molecule at Zn_A in the initial structure in Fig. 1 has dissociated to a hydroxide ion that bridges Zn_A and Zn_B and a proton that has been transferred to O8 of Glu27. The Zn–Zn distance in compound **1** is 3.28 Å, and the respective distances of Zn_A and Zn_B from the hydroxide oxygen are 1.92 and 1.93 Å. Optimization of the complex in Fig. 1 without the water molecule yields compound **2** (Fig. 3),

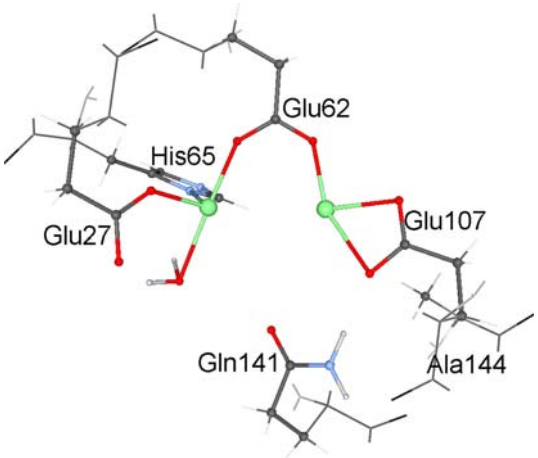

Fig. 1 Initial configuration of the dizinc ferroxidase model center with component amino acids labeled. Atomic coordinates are from Protein Data Bank file 2CEI [2]. Oxygen atoms are *red*, carbon atoms *dark gray*, nitrogen atoms *light blue*, hydrogen atoms *white*, and zinc ions *light green*

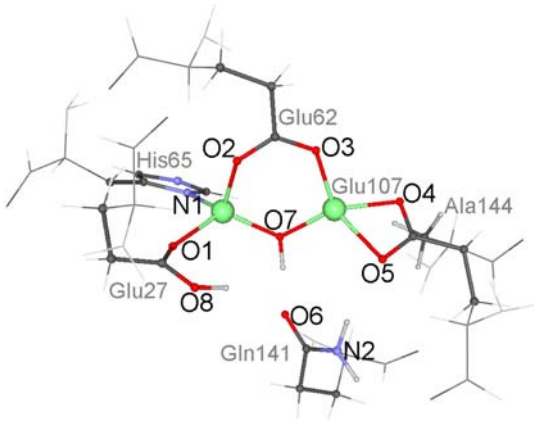

Fig. 2 Compound **1**, the result of BPW91/DNP optimization of the geometry of the initial configuration in Fig. 1. The hydroxide bridge and protonated O8 of Glu27 resulting from dissociation of the water molecule of the initial configuration are seen. Atom numbers shown are referred to throughout the text

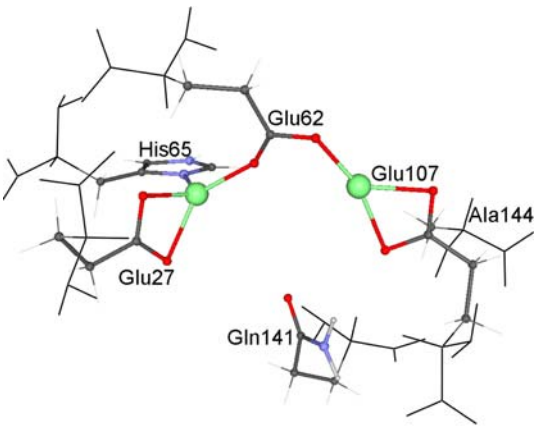

Fig. 3 Coordination at the metal centers in compound **2**, the result of optimization of the configuration in Fig. 1 omitting the water molecule at Zn_A. The Zn–Zn distance is 4.79 Å

and comparing the energy of **2** plus an isolated water molecule (Table 1) with that of **1** indicates a substantial net binding energy for the bridged, protonated complex of 44.2 kcal/mol. The optimization leading to compound **1** demonstrates that a hydroxide bridge can form readily within the ferroxidase center by dissociation of a water molecule, and that said water molecule need not initially be very near the bridging position for that to occur.

The presence of the hydroxide bridge goes far toward explaining both the short Zn–Zn separation and the position of the amide oxygen of Gln141 in the experimental structure [2]. The Glu62 carboxylate bridge alone does not constrain the metal ions much. In compound **2**, where it is the only bridge, the Zn–Zn distance is 4.79 Å. Gln141 does seem to bridge sites A and B through hydrogen bonds from its amide nitrogen to the Glu107 carboxylate at site B and

Table 1 Energy and structure data for optimized compounds

Compound	Figure	Energy	MAD (Å)	MAX (Å)	DIH (°)	No. of H_2O	Tyr/Ala
Zn^{2+}		–1,778.62364					
H_2O		–76.46035					
OH^-		–75.79970					
Glu27		–475.98262					
Tyr34		–554.92173					
Glu62		–475.98232					
His65		–473.65696					
Glu107		–475.98264					
Gln141		–456.64919					
Ala144		–248.56560					
1	2	–6,242.36154					
2	3	–6,165.83079					
3		–6,241.97150					
4	4, 5	–6,318.45252	0.32	1.06 (O4)	120.2	1	
5		–6,318.44868	0.32	1.15 (OH_2)	120.3	1	
6		–6,394.91688	0.39	0.95 (O4)	116.7	2	
7		–6,949.84368	0.36	0.80 (O2)	129.0	2	+Y
8	6	–6,949.84495	0.36	0.67 (O3)	120.9	2	+Y
9		–6,949.84827	0.37	1.24 (O4)	124.3	2	+Y
10		–6,394.92250	0.30	0.60 (O3)	162.4	2	
11	8	–6,394.92036	0.27	0.60 (OH_2)	174.6	2	
12		–6,394.91860	0.35	0.76 (O4)	143.2	2	
13	7	–6,394.92374	0.42	1.32 (O8)	146.7	2	
14		–6,949.84512	0.35	1.06 (O3)	145.9	2	+Y
15		–6,949.85396	0.47	1.28 (O8)	147.9	2	+Y
16		–6,394.92069	0.37	0.77 (O3)	132.5	2	
17		–6,394.91980	0.30	1.02 (O4)	121.8	2	
18		–6,873.37690	0.34	0.73 (O3)	125.1	2	+Y
19		–6,949.84843	0.26	0.56 (OH_2)	170.4	2	+Y
20	9	–6,949.84573	0.25	0.56 (N2)	170.4	2	+Y
21		–6,701.28537	0.26	0.55 (OH_2)	170.0	2	+Y, –A
22		–6,701.28260	0.25	0.55 (N2)	168.8	2	+Y, –A
23		–7,026.30556	0.38	2.44 (O2)	177.6	3	+Y
24		–7,026.30372	0.40	3.11 (O2)	177.6	3	+Y
25		–7,026.32662	0.44	2.64 (O2)	179.2	3	+Y
26		–6,471.39623	0.41	0.89 (O4)	131.6	3	
27		–7,026.32388	0.41	1.06 (O3)	140.7	3	+Y
28		–7,026.31756	0.34	0.73 (O3)	170.8	3	+Y

Total energies are in atomic units (1 au = 627.5095 kcal/mol)

MAD mean absolute deviation, *MAX* maximum deviation, *DIH* dihedral angle

from its amide oxygen to the water molecule at site A [2]. But the latter is a relatively weak hydrogen bond (experimental O–O distance 3.00 Å), and some additional structural element is needed to explain the observed Zn–Zn separation. By way of comparison, the dimagnesium ferroxidase complex of FrMF does appear to possess only a hydrogen-bonding network bridging the centers, and in this the Mg–Mg separation is 4.0 Å [9].

The hydroxide bridge also rationalizes well the position of the amide oxygen of Gln141, which lies midway between the metal ions but is coordinated directly to neither. Gln141 is a site B ligand and might be expected to

Table 2 Compound **20**: experimental and calculated bond lengths (Å) and angles (°)

Bonds	Bond lengths (Å)		Bonds	Bond angles (°)	
	Calculated	Experimental[a]		Calculated	Experimental[a]
Zn–Zn	3.412	3.330	H_2O–Zn–O2	162.2	172.0
N1–Zn	2.108	2.294	N1–Zn–O1	110.0	110.3
H_2O–Zn	2.157	2.333	H_2O–Zn–O1	92.6	86.9
O2–Zn	2.418	2.066	N1–Zn–O2	101.2	93.5
O6–Zn	3.836	3.824	N1–Zn–Zn	115.3	107.7
O7–Zn	1.999		O1–Zn–Zn	121.3	136.3
O3–Zn	2.025	1.961	H_2O–Zn–Zn	116.7	110.9
O4–Zn	2.187	2.160	O2–Zn–Zn	58.6	67.0
O5–Zn	2.194	2.310	O3–Zn–O4	91.5	92.0
O6–Zn	4.123	3.966	O3–Zn–O5	150.5	144.4
O7–Zn	1.952		O4–Zn–O5	60.5	58.2
TyrO–O4	2.834	2.728	Zn–O6–Zn	50.6	50.6
N2–O5	2.973	2.788	Zn–O2–O3–Zn	29.8	5.5

[a] From [2]

coordinate to Zn_B. In FrMF [9] the Gln141 amide oxygen is indeed 0.6 Å closer to site B than to site A. In compound **1** it hydrogen-bonds to the hydroxide, and the bond length of 1.61 Å indicates a rather strong bond. In this position it is 3.97 Å from Zn_A and 3.93 Å from Zn_B, in good agreement with the crystallographic Zn–O distances (Table 2) of, respectively, 3.82 and 3.97 Å. Bridging oxygens have also been observed in the EcFtnA Fe^{3+} and Zn^{2+} ferroxidase complexes [8], and these feature short metal–metal separations and a centrally directed glutamine oxygen. Overall, the high exothermicity of hydroxide bridge formation, the absence of a kinetic barrier, and complete consistency of the bridge with the crystallographic structure overwhelmingly favor the likelihood of its presence in the complex.

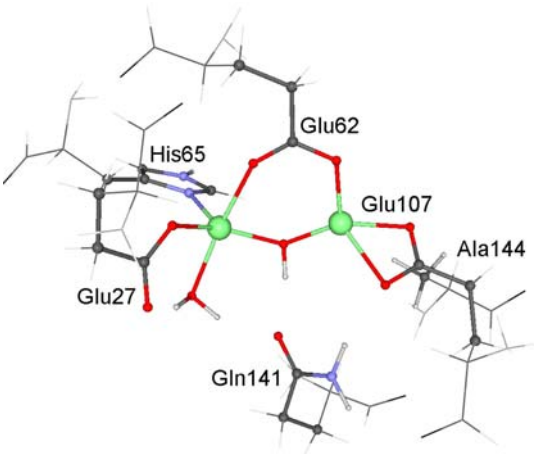

Fig. 4 Optimized structure of compound **4**, an electrically neutral complex that reproduces the experimental [2] ligand arrangement around Zn_A. The water molecule forms hydrogen bonds to O8 of Glu27 and O6 of Gln141, and the latter also accepts a hydrogen bond from the bridging hydroxide

Configuration at site A

When the proton is removed from O8 of **1**, a neutral complex results that is optimized to compound **3**. Adding a water molecule back to **3** in the original experimental position (see Fig. 1) gives compound **4** (Fig. 4) upon optimization. The binding energy of the added water is 13.0 kcal/mol (Table 1). Compound **4** reproduces well the experimental structure at site A; site B is discussed below. Figure 5 displays the structure of **4** superimposed on the experimental structure. The Zn–Zn axis in the calculated structure is tilted (by 8.4°) with respect to the experimental structure. This axial tilt seems to arise from the combination of the basic geometric constraints of the complex and the fact that the BPW91 C–O bond lengths in the Glu62 carboxylate are too long by about 0.05 Å.

In **4** Zn_A is five-coordinate, with ligands arranged approximately trigonal bipyramidally. The water oxygen and O2 of Glu62 are axial. The equatorial angles are 110.0°, 101.5°, and 146.9°. The latter angle, HO–Zn–N1, is open enough to provide a possible additional coordination position. The Glu62 carboxylate, the zinc ions, and the water oxygen are approximately coplanar, and this plane conveniently partitions the coordination environment into hemispheres. The hydroxide bridge is out of the plane by 24°, and the hemisphere occupied by it will be referred to as the lower, or "down," hemisphere, while ligands on the opposite side are "up." The water molecule is not only securely bound to Zn_A, it is also hydrogen-bonded to O8 of Glu27 and O6 of Gln141. A complex, compound **5**, was optimized that differs from **4** in that the water, in a conformation similar to that shown in Fig. 1, hydrogen-bonds only to O8. Without the hydrogen bond to O6, the arrangement of the site A ligands compares more poorly to

the experimental arrangement, but compound **5** is only 2.4 kcal/mol higher in energy than **4**.

Agreement between calculated and experimental structures was measured by the mean absolute deviation and by the maximum deviation of the atomic positions of the 54 atoms present in the crystallographic structure that were allowed to float in the DFT optimizations. Mean absolute deviation and maximum deviation values for relevant compounds are displayed in Table 1. A low mean absolute deviation and a narrow range of deviations among the atoms directly coordinated to the metal ions are both elements of satisfactory agreement. Secondarily, a satisfactory maximum deviation should apply to an atom of one of the weakly bound groups, the amide oxygen (O6) or nitrogen (N2) of Gln141 or the oxygen of the site A water molecule. Close agreement between the experimental and calculated geometries is not necessarily to be expected. Besides the random errors in experimental atomic positions and the systematic error inherent in geometry optimizations done with a specific theoretical method, finite basis sets, and a given model, there remains the fact that theoretically derived geometries are directly applicable to molecules in the gas phase at low temperature and do not account for crystal packing and other solid-state effects.

Configuration at site B

In compound **4** (Fig. 5) the Glu107 carboxylate oxygens are seen to be rotated with respect to their positions in the experimental structure. The dihedral angle O3–Zn–O4–O5 is 159.4° in the experimental structure and 120.2° in **4**. This dihedral angle is used throughout as an approximate measure of rotation of the Glu107 carboxylate. In **4** the observed rotation brings the ligands nearer tetrahedral coordination, and would be unremarkable in a complex with a four-coordinate metal. The experimentally observed flattening of the carboxylate therefore suggests a higher coordination number at site B. There are two potential open coordination positions at Zn_B, one each in the upper and lower hemispheres of the complex.

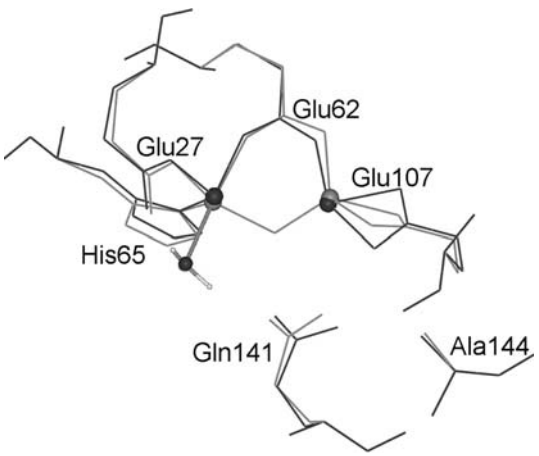

Fig. 5 Line representation of compound **4** (*gray*) superimposed on the experimental geometry (*black*). The rotation of the Glu107 carboxylate discussed in the text is evident

Although the crystal structure of the wild-type ferroxidase center does not show a water molecule at site B, that of the Glu27Asp mutant (PDB 2CIH) [2] does have a water in a down coordination position. Compounds **6–9**, initiated with a water in various orientations below the plane, were optimized to explore the structural effect of water in this position. In **6–8** the water molecule hydrogen-bonds to the hydroxide oxygen, which is the most negative oxygen in the complex. In **9** the water molecule is hydrogen-bonded to O4, which is no longer bonded to Zn. In none of compounds **6–9** is the rotation of the Glu107 carboxylate corrected or even altered significantly, and large deviations in the positions of the Glu107 oxygen atoms remain. The dihedral angle in the experimental PDB 2CIH geometry is 141.9°, so it exhibits rotation as well, although there is clearly an additional influence that lessens the rotation.

A water molecule added to Zn_B in the up position results in a flattened Glu107 carboxylate (Table 1) in each of compounds **10–17**. The up position offers more potential hydrogen-bonding opportunities than does the down position. Oxygen atoms O1–O5 and O8 are available, and structures were optimized in which water hydrogen-bonds to each of these, except for O4. O4 seems to be unavailable because water in a position to hydrogen-bond to it is also in a position to hydrogen-bond to either O3 or O5, which are preferred.

In compounds **10** and **11** water hydrogen-bonds to O2. The two differ essentially only in rotation of the water about the hydrogen bond. Compound **11** is displayed in Fig. 6. In **12** the water breaks the O5–Zn bond and bonds to both atoms. O5 is hydrogen-bonded to N2 of Gln141, and N2 deviates substantially from its experimental position in this compound. Compound **13** (Fig. 7) is the global minimum energy structure. Its water at Zn_B is strongly hydrogen bonded to O8 of Glu27, and pulls this atom away from its observed position. Compound **15** is quite similar to **13**. In **14** water hydrogen-bonds to O3 of Glu62, causing a large deviation in the position of that atom. The water molecule at Zn_B in compound **16** hydrogen-bonds to O1 of Glu27 and secondarily to O3 of Glu62, inducing deviations in both Glu107 oxygens. In **17** the water molecule is not attached to Zn_B at all. It is hydrogen-bonded to O3 of Glu62, and the Glu107 carboxylate exhibits the expected rotation toward the tetrahedral.

The closely related compounds **10** and **11** feature relatively low mean absolute deviations and a narrow range in deviations of atoms attached to the metal ions. In **11** the maximum deviation occurs in the oxygen of the site A

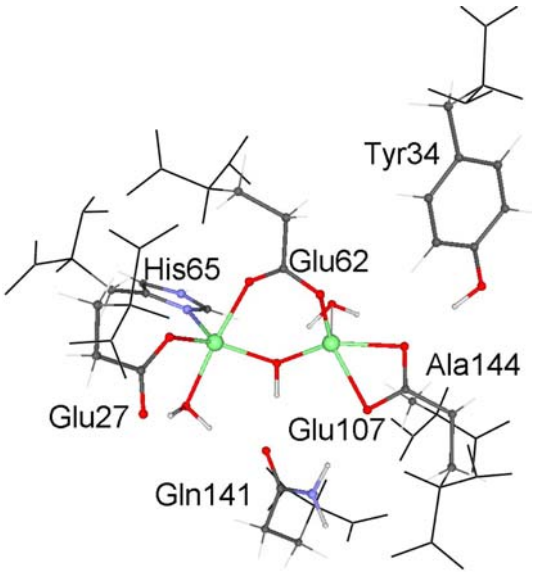

Fig. 6 Compound **8** showing Tyr34 in a position to hydrogen-bond to O4 of Glu107 and a water molecule at Zn_B in the down position and hydrogen-bonded to hydroxide

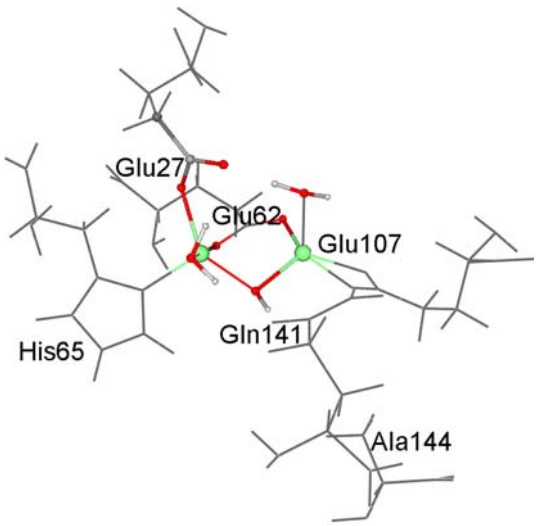

Fig. 7 The structure of compound **13**, the global minimum energy structure in complexes without Tyr34, shown mostly in line representation, with the water molecule at Zn_B in the up position hydrogen-bonded to O8 of Glu27

water molecule. Both feature a flat dihedral angle. Neither **10** nor **11** is the global minimum energy structure, nor are they substantially more stable than **6–9**, the compounds in which the water molecule at site B is in the down position. Nevertheless they provide the best representations of the structure of PDB 2CEI.

Both Zn_A and Zn_B are five-coordinate in the best optimized geometries, each with one water molecule in its primary coordination sphere. Double pentacoordination is also reasonable for the analogous diiron(II) complex, to which a molecule of dioxygen will be attached to form a peroxide bridge between the metal centers as the ferroxidase reaction proceeds. Although primary coordination in HuHF has not been defined experimentally, it has been for FrMF. A recent magnetic circular dichroism spectroscopic study of the diiron(II) ferroxidase complex in FrMF determined that both irons are five-coordinate [34]. The FrMF complex showed no evidence of hydroxide bridging, which appears to be a feature of the dizinc HuHF ferroxidase complex. FrMF has an aspartate at position 144, so it is electrically neutral without a hydroxide.

Tyrosine 34

Tyr34 is near enough to the ferroxidase center to interact via a hydrogen bond to O4 of Glu107, and that fact has prompted investigations of its effect on ferroxidase activity. Kinetics studies have compared the rate of ferroxidation [35, 36] with Tyr34 present with that when it is replaced by phenylalanine. The rates in the absence of tyrosine have been found to drop, but by less than 100-fold. Although Tyr34 affects the rate of reaction, it is not necessary for ferroxidase activity [15]. The structural effect of Tyr34 was examined by including it in more than half the complexes listed in Table 1, its presence being indicated in the rightmost column.

In an initial test Tyr34 was added to **4** (Fig. 4), a complex with no water molecule at site B, and one that exhibits rotation of the Glu107 carboxylate (dihedral angle 120.2°). Optimization yields compound **18**, which features a hydrogen bond from the Tyr34 hydroxide to O4. Tyr34 improves the rotation of the Glu107 carboxylate slightly, to a dihedral angle of 125.1°.

Tyr34 was added to **10** and **11** to give, respectively, compounds **19** and **20**. Compound **20** is shown in Fig. 8, Fig. 9 displays it superimposed on the experimental structure, and Table 2 compares calculated and experimental bond lengths and angles. In both **19** and **20** the addition of tyrosine slightly improves agreement with experiment as measured by both the mean absolute deviation and the maximum deviation (Table 1). Again the primary interaction is through a weak hydrogen bond to O4 of Glu107. The interaction energies (Table 1) between Tyr34 and **19** and **20**, are, respectively, −2.6 and −2.3 kcal/mol. These are consistent with the observed kinetic effects, which indicate a change in activation energy of less than 3 kcal/mol, assuming similar reaction coordinates, when tyrosine is replaced. Tyr34's weak attraction slightly improves the agreement between calculated and experimental structures.

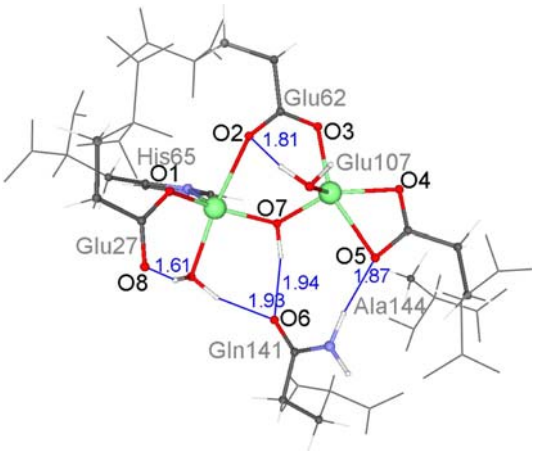

Fig. 8 Compound **11**, the best fit to the experimental structure among complexes not including Tyr34. The water molecule at Zn_B in the up position is hydrogen-bonded to O2 of Glu62. Several hydrogen bond lengths (Å) are indicated

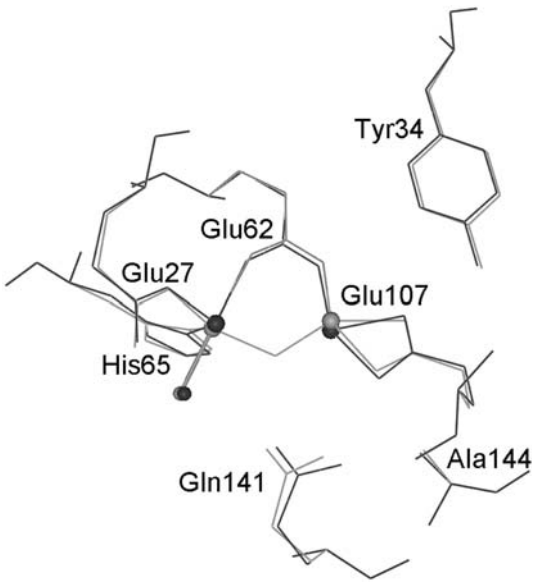

Fig. 9 Line representation of compound **20** (*gray*), compound **11** with Tyr34 added, superimposed on the experimental structure (*black*) of dizinc ferroxidase

Alanine 144

Whether Ala144 affects ligand geometry at all at site B through some steric effect or is simply an inert ligand is unclear. The aspartate and glutamate, respectively, at the corresponding positions in FrMF and EcFtnA are active in metal binding. Research on the Ser144Ala mutation in MtF [10, 16], has led to the view that, because the residue at the 144 position intrudes into the path between the outer surface of the subunit and site B, the small, inert alanine permits freer access of the metal to site B. This interpretation indicates that alanine is an inert placeholder that has little structural effect on ferroxidase complexes.

The interaction energy of alanine with the dizinc ferroxidase complex was examined by removing Ala144 from compounds **19** and **20** and reoptimizing to obtain compounds **21** and **22**. The energies of **21** and **22**, respectively, plus that of isolated alanine (Table 1) can be compared with those of **19** and **20** to arrive at the interaction energies. The calculated interaction energies of 1.59 and 1.55 kcal/mol, respectively, are small and repulsive. Therefore, Ala144, although in the primary ligand sphere, interacts more weakly with the rest of the complex than does Tyr34 in the secondary ligand sphere. Removal of alanine has a negligible effect on the geometry of the complex, and thus the interaction energy calculations tend to support the placeholder role indicated by the kinetics experiments [10].

The effect of an additional water molecule

The experimental structure is well reproduced by a model in which each zinc ion has one ligand water molecule in its primary coordination sphere. Before concluding that the structure of the complex of PDB 2CEI contains only two water molecules, it is important to examine whether an additional water molecule could attach to either the primary or the secondary sphere to form a stable complex and whether such attachment would perturb the structure enough to be noticeable in the crystal structure. Three sample calculations for each site were performed in which a single additional water molecule was added to previously optimized complexes. A water added to site A of compound **19** produced compound **23** and addition in two orientations to **20** yielded compounds **24** and **25**. In compounds **23** and **24** the added water attached to Zn_A, in the process displacing O2–Glu62, which rotated about 90° to hydrogen-bond to the water molecule on Zn_B. Thus, Zn_A remains pentacoordinate, and neither of the substituted complexes is as stable as the one it replaced. In compound **25** the added water molecule does not bind to zinc but hydrogen-bonds to O3 of Glu62, leaving Zn_A. The loosely attached water molecule has a binding energy of −12.9 kcal/mol. Glu62 again separates from Zn_A, rotates 90°, and hydrogen-bonds to the water at Zn_B.

Adding a water molecule at the open site B position of, respectively, compounds **12**, **19**, and **20** yielded compounds **26**–**28**. In none of these did the water bind to zinc. Zn_B remained pentacoordinate. In each case water migrated to hydrogen-bond to the hydroxide oxygen, which is the most negative in the ferroxidase complex. Each of the added water complexes is stable with respect to reactants. In compound **28** the oxygen atom of the added water is coordinated loosely (O–H distance 2.06 Å) with a hydrogen on the histidine imidazolyl ring. In compound **26** the

first water molecule at site B is hydrogen-bonded to O1, and the second is nearly the same as in compound **28**. In compound **27** the first water switches its hydrogen bond from O2 to O1, and the dihedral angle changes as a result.

The addition of a water molecule, even in secondary positions, produced noticeable effects on the primary ligand positions. Thus, although only a limited number of configurations were examined, these indicate that the crystallographic structure would have betrayed the presence of water molecules in the secondary coordination sphere; therefore, the PDB 2CEI structure does not appear to possess more than two water molecules. The loosely bound extra water molecules form stable complexes, and so structures with more waters are to be expected. In fact, in the Glu27Asp mutant (PDB 2CIH) a secondary water does appear.

Summary

DFT calculations on a compact model of an HuHF ferroxidase–dizinc complex have been found to represent the structure faithfully. The crystallographic structure [2] locates the zinc ions and several water molecules in the wild type and in mutated centers, permitting the primary coordination spheres of the two metal ions to be defined in geometry-optimization calculations. The calculations in turn serve as a commentary on the structure presented in PDB 2CEI, and they bring out features implicit in the experimental structure. The complex is electrically neutral as expected in a low-effective-dielectric medium such as a protein. The metal ions are pentacoordinate, each with one water molecule ligand, and the centers are bridged by a hydroxide ion. The siting of the amide oxygen of Gln141 about equidistant from the metal ions fits well with the location calculated for the hydroxide. At site A of the complex the orientation of the water ligand emerges clearly because both hydrogen atoms bond to neighboring oxygen atoms. Two closely related isomers represent site B, and both may be present in the crystallographic structure. Several complexes differing in the position of water molecules lie within 10 kcal/mol in energy of the structures that agree most closely with the experimental structure. The potential energy surface of the ferroxidase center thus appears to be complex, with a water structure that confers the ability to adapt to changes in the ligand environment. This view is borne out in the crystallographic depiction [2], in which each structure has slight differences in water number and position.

Pentacoordination of the metal centers has been noted in a recent magnetic circular dichroism spectroscopic study of the diiron(II) ferroxidase complex in FrMF [34], although that complex has no hydroxide bridge. Thus, if the dizinc complex accurately models the diiron(II) in HuHF, interesting variations in the initial HuHF and FrMF ferroxidase complexes may be present.

Acknowledgments The authors gratefully acknowledge the support of this research by the National Science Foundation in the form of grant no. MCB-0641269. D.E.B. is grateful for support from the Consejo Nacional de Investigaciones Científicas y Técnicas de la República Argentina.

References

1. Pau MYM, Lipscomb JD, Solomon EI (2007) Proc Natl Acad Sci USA 104:18355–18362
2. Toussaint L, Bertrand L, Hue L, Crichton RR, Declercq JP (2007) J Mol Biol 365:440–452
3. Liu X, Theil EC (2005) Acc Chem Res 38:167–175
4. Chasteen ND, Harrison PM (1999) J Struct Biol 126:182–194
5. Zhao G, Su M, Chasteen ND (2005) J Mol Biol 352:467–477
6. Bou-Abdallah F, Arosio P, Santambrogio P, Yang X, Janus-Chandler C, Chasteen ND (2002) Biochemistry 41:11184–11191
7. Treffry A, Zhao Z, Quail MA, Guest JR, Harrison PM (1997) Biochemistry 36:432–441
8. Stillman TJ, Hempstead PD, Artymiuk PJ, Andrews SC, Hudson AJ, Treffry A, Guest JR, Harrison PM (2001) J Mol Biol 307:587–603
9. Ha Y, Shi D, Small GW, Theil EC, Allewell NM (1999) J Biol Inorg Chem 4:243–256
10. d'Estaintot BL, Santambrogio P, Granier T, Gallois B, Chevalier JM, Précigoux G, Levi S, Arosio P (2004) J Mol Biol 340:277–293
11. Lawson DM, Artymiuk PJ, Yewdall SJ, Smith JMA, Livingstone JC, Treffry A, Luzzago A, Levi S, Arosio P, Cesareni G, Thomas CD, Shaw WV, Harrison PM (1991) Nature 349:541–544
12. Hempstead PD, Hudson AJ, Artymiuk PJ, Andrews SC, Banfield MJ, Guest JR, Harrison PM (1994) FEBS Lett 350:258–262
13. Hempstead PD, Yewdall SJ, Fernie AR, Lawson DM, Artymiuk PJ, Rice DW, Ford GC, Harrison PM (1997) J Mol Biol 268:424–448
14. Pearson RG (1963) J Am Chem Soc 85:3533–3539
15. Liu X, Theil EC (2004) Proc Natl Acad Sci USA 101:8557–8562
16. Bou-Abdallah F, Santambrogio P, Levi S, Arosio P, Chasteen ND (2005) J Mol Biol 347:543–554
17. Friesner RA (2007) Proc Natl Acad Sci USA 102:6648–6653
18. Siegbahn PEM, Borowski T (2006) Acc Chem Res 39:729–738
19. Siegbahn PEM (1999) Inorg Chem 38:2880–2889
20. Friesner RA, Guallar V (2005) Annu Rev Phys Chem 56:389–428
21. Ramos MJ, Fernandes PA (2008) Acc Chem Res 41:689–698
22. Guallar V, Jacobson M, McDermott A, Friesner RA (2004) J Mol Biol 337:227–239
23. Mitic N, Clay MD, Saleh L, Bollinger JM, Solomon EI (2007) J Am Chem Soc 129:9049–9065
24. Han WG, Liu T, Lovell T, Noodleman L (2006) Inorg Chem 45:8533–8542
25. Schwartz JK, Wei P, Mitchell KH, Fox BG, Solomon EI (2008) J Am Chem Soc 130:7098–7109
26. Han WG, Noodleman L (2008) Inorg Chem 47:2975–2986
27. Rinaldo D, Philipp DM, Lippard SJ, Friesner RA (2007) J Am Chem Soc 129:3135–3147
28. Bacelo DE, Binning RC (2006) Inorg Chem 45:10263–10269
29. Hwang J, Krebs C, Huynh BH, Edmondson DE, Theil EC, Penner-Hahn JE (2000) Science 287:122–125
30. Becke AD (1988) Phys Rev A 38:3098–3100

31. Perdew JP, Burke K, Wang Y (1996) Phys Rev B 54:16533–16539
32. Delley BJ (1990) Chem Phys 92:508–517
33. Delley BJ (2000) Chem Phys 113:7756–7764
34. Schwartz JK, Liu XS, Tosha T, Theil EC, Solomon EI (2008) J Am Chem Soc 130:9441–9450
35. Fetter J, Cohen J, Danger D, Sanders-Loehr J, Ha Y, Theil EC (1997) J Biol Inorg Chem 2:652–661
36. Bauminger ER, Harrison PM, Hechel D, Hodson NW, Nowik I, Treffry A, Yewdall SJ (1993) Biochem J 296:709–719